A generalized disjunctive programming model for multi-stage compression for natural gas liquefaction processes.

Fahad Matovu[1,*], *Shuhaimi* Mahadzir[1,2,**], and *Nor Erniza Mohammad* Rozali[1,***]

[1]Chemical Engineering Department, Universiti Teknologi Petronas, 32610, Perak, Malaysia.

[2]Centre for Systems Engineering, Institute of Autonomous System, Universiti Teknologi Petronas, Malaysia.

Abstract. The primary driver of operating costs in natural gas processes is the energy consumption of the compression system. Multistage compression configurations are commonly employed and hence play a vital role in optimization of natural gas processes. In this study, a generalized disjunctive programming model for multistage compression is formulated. The model is useful for both synthesis and optimization of multistage compression configurations. By using this approach, we further seek improvements in shaft work savings. The model relies on thermodynamic equations and is designed to minimize the consumption of shaft work. The model is handled by employing the logic-based branch and bound algorithm, eliminating the need for explicit conversion into a MINLP, which in turn leads to improved convergence and faster computational performance. The model solution yields optimal pressure levels, and hence stage shaft work consumptions. A case study of multistage compression for a prior optimized single mixed refrigerant (SMR) process obtained from literature is used to test the proposed model. The model's outcomes are validated through simulation using the Aspen Hysys software. Savings in shaft work of atmost 0.0088%, 0.4433%, and 1.2321% are obtained for the two, three, and four stage compression systems respectively against the optimized base cases from literature.

1 Introduction

Natural gas (NG) is recently considered as a potent and clean energy source due to production of low carbon emissions in comparison to other fossil fuels [1]. Due to the demand for environmentally benign energy sources, natural gas has received increasing attention in recent years. Natural gas demand is expected to grow by 60% between 2010 and 2030, and is anticipated to surpass coal as a dominant energy provider by approximately 2035 [2]. In industrial applications where gas is transported through pipelines, one of the most crucial processes is gas compression. It is commonly employed in internal combustion engines, power generation cycles, domestic gas supply and refrigeration cycles [3–5].

*e-mail: mfahd57@gmail.com
**e-mail: shuham@utp.edu.my
***e-mail: erniza.rozali@utp.edu.my

Keywords:

Multistage compression; Generalized disjunctive programming; Natural gas; Liquefaction processes

The majority of natural gas resources are located in distant and isolated areas. This necessitates their transportation over extended distances. The transportation of natural gas in its gaseous state poses difficulties due to its significant volume and the risk of flammability. The most efficient method for long distance transport involves the liquefaction of natural gas in industrial refrigeration facilities. This process involves cooling the natural gas to -160 °C to produce liquefied natural gas (LNG) at atmospheric pressure. This reduces its volume to one six hundredth of its original volume and mitigates the explosion risk [2]. Nonetheless, the liquefaction process demands a substantial amount of energy. This constitutes approximately 40% to 60% of the overall cost of LNG production [6] and roughly 30% of the total energy consumed within the natural gas value chain [2]. Consequently, it is of utmost significance to optimize these processes in order to enhance energy efficiency and reduce associated expenses to a minimum. However, the mechanistic and thermodynamic models required to accurately describe liquefaction processes are complex, highly non-linear and non-convex. This complicates the optimisation challenge [1] [7]. Nevertheless, many studies have focused on this considerable task using a variety of techniques that range from deterministic to stochastic algorithms.

In the realm of deterministic optimization techniques, sequential quadratic programming (SQP) was employed by several researchers. Khan et al. [8] used SQP to optimize the single mixed refrigerant (SMR) process, Wahl et al. [9] applied it to the Poly Refrigerant Integral Cycle Operation (PRICO) LNG process, and Hwang et al. [10] utilized SQP for the dual mixed refrigerant (DMR) process. Mussati et al. [11] optimized a series flow double-effect water-lithium bromide absorption refrigeration system using the generalized reduced gradient algorithm to minimize costs. On the other hand, when it comes to stochastic optimization techniques, Shirazi and Mowla [12] utilized the genetic algorithm (GA) to minimize the total energy consumption in an SMR process of an LNG peak shaving plant. Khan and Lee [13] utilized the particle swarm optimization (PSO) technique to enhance energy efficiency in an SMR process. Primabudi et al. [14] adopted the non-dominated sorting genetic algorithm II (NSGA-II) to perform multi-objective exergoeconomic optimization for a C3MR LNG plant. Alabdulkarem et al. [15] harnessed the genetic algorithm from the Matlab optimization toolbox for optimizing a propane pre-cooled mixed refrigerant (C3MR) LNG plant. Meanwhile, Aspelund et al. [16] devised a gradient-free optimization-simulation approach based on Tabu Search (TS) and the Nelder-Mead Downhill Simplex (NMDS) to minimize energy consumption in a PRICO process integrated into Aspen Hysys. Almeida-Trasvina et al. [17] introduced structural modifications to a novel SMR process and minimized shaft work consumption employing the genetic algorithm.

Due to the fact that the energy consumption of these processes is attributed to the compressor configuration, we extend the analysis of optimization of such processes to the compressor configurations. In addition, the total operational expenses of an LNG facility are dominated by the energy requirement for refrigerant compression [17]. Various works have considered single, two, three or four stage compressor configurations separately in the analysis and/or optimization of LNG processes with the exception of a few works such as Tak et al. [18] who consindered two, three and four, and Ebrahimi et al. [19] one and four stages. Forexample Lee et al. [20], Aspelund et al. [16], Wahl et al. [9] considered one stage compression configurations. Shirazi and Mowla [12], He et al. [21], Aslambakhsh et al. [22], and Lee and Moon [23], Li and Ju [24] considered two and three stages respectively. Others such as Khan and

Lee [13], Qadeer et al. [25], Qyyum et al. [26] considered four stage compression cycles. It is clear that consideration of the number of compression stages is an important factor for the synthesis and optimization of natural gas liquefaction processes. Nevertheless, there is less focus on research that investigates simultaneously different compressor configurations in the synthesis and optimization analysis of LNG cycles to improve their energy efficiency. In addition, there is need for a robust and quick approach that considers the number of compression stages while optimizing liquefaction processes. This may be useful at all stages of synthesis and optimization of liquefaction processes, at start-up design stages or retrofits. Also, the problem formulations are highly nonlinear and non-convex, and hence their solution still pose significant challenges. Therefore, improvements and/or alternative view points of approach are still welcome.

This work develops a novel generalized disjunctive programming (GDP) model for multistage compression configurations. Raman and Grossmann [27] introduced the GDP paradigm which presents models using algebraic equations, boolean and continuous variables, disjunctions and logic propositions. This has been applied in a variety of applications that include operations planning and scheduling, synthesis of flowsheet and reactor networks, process control and others [28]. Modeling and optimization of the problem as a GDP further benefits the approach by making the modelling easier to understand since it retains the underlying logical relationships; obtaining improved robustness and convergence speed while applying logic-based solution techniques to solve the problem [29]; and having access to a variety of solution approaches [30] [31]. The model relies on thermodynamic equations and is designed to minimize the consumption of shaft work. The model is useful for optimization of processes with multistage compression configurations. In addition, it also considers synthesis where different number of compressor configurations are considered. This work also aims to explore alternative promising directions for further study of optimization applied to LNG refrigeration cycles. In this case, the problem is redefined and approached using a different perspective not explored before. This enhances the capacity to solve the mathematical models efficiently and rigorously. A case study of multistage compression for a prior optimized SMR process as obtained from literature, is employed to evaluate the proposed model. The results obtained are confirmed through validation using Aspen Hysys software, offering a sense of assurance in the achieved solutions.

2 Materials and Methods

2.1 Process description and configurations

2.1.1 Process description of mixed refrigerant (MR) cycles

The natural gas liquefaction cycles mainly comprise of compression and expansion of the refrigerant. A fascinating MR cycle known as the "self-cooling" cycle is displayed in Figure 1. In this cycle, the natural gas is cooled down in a multistream heat exchanger (MHEX) and expanded to a pressure of about 1 atm to form LNG. In the MR cycle, the refrigerant at high pressure, as it exits the compressor, dissipates heat to an external heat reservoir. It then rejects heat to the low pressure refrigerant obtained after expanding the high pressure refrigerant in the JT valve. The heat rejection process ensures that the hot refrigerant undergoes additional cooling, potentially leading to subcooling, before undergoing expansion. It also makes the obtained low pressure refrigerant attain a lower temperature and vapour fraction. The drawback of this however is an increase in heat exchanger duty and hence heat transfer area is also increased [32]. The natural gas and high pressure streams correspond to the hot streams of the MHEX. The low pressure stream corresponds to the cold stream of the MHEX.

For actual natural gas processes, the compression stage shown in Figure 1 is normally a multistage compression system coupled with intercooling as shown in Figure 2. These processes encounter large pressure differences between the inlet and outlet pressures. Therefore, for compression systems from a given pressure P_{min} to much higher pressure P_{max}, the compression is split into smaller stages. For each intermediate stage, the gas undergoes compression at a specific intermediate pressure level. Afterward, it experiences cooling and is directed towards the inlet of the subsequent stage's compressor. This cycle continues repeatedly until the desired process exit pressure P_{max} is reached. Despite this procedure not being ideal, employing a multi-stage compression approach can yield substantial savings. The extent of these savings hinges on the number of stages involved in the entire compression process and the distribution of the total pressure ratio $\mathcal{PR}_{tot} = P_{max}/P_{min}$ across these individual stages. An ideal isothermal process results in minimum work for compression. However, an infinite number of intercoolers is required in this case. Under actual circumstances, the compression ratio is divided into two or more stages with cooling the compressed gas in between stages. This is done for design reasons and in attempts to consume minimum shaft work energy [4]. The number of stages is governed by economics whereas the total pressure ratio distribution is a technical issue [33]. Generalized disjunctive programming is employed in this work to address these two issues.

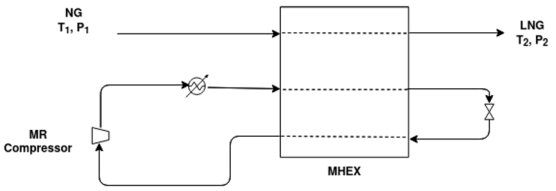

Figure 1: A self-cooling MR cycle.

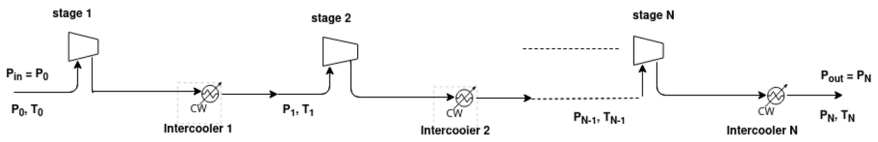

Figure 2: Multistage compression with intercooling.

2.1.2 Single mixed refrigerant (SMR) compression configurations

For liquefaction processes, the refrigerant in gaseous form is compressed in compressors resulting in exiting gas with higher specific volumes and increasingly higher temperatures [18]. In order to lower exit temperatures, decrease gas specific volumes and hence lower compressor power consumption, intercooling is employed. Thus, multistage compression with intercooling is commonly employed in natural gas liquefaction processes. SMR processes of various compression configurations are shown in Figure 3. The sub-figures show two, three and four compression stage systems respectively. Note that a one stage compression system is shown in Figure 1. Each process consists of a multistream heat exchanger (MHEX), compressor(s), cooler(s) and Joule Thomson (JT) valve(s).

Natural gas enters the LNG MHEX at a high pressure and room temperature, where it exchanges its latent heat of vaporization/condensation with the cold MR stream. It exits the MHEX as a subcooled liquid at elevated pressure. It then undergoes flashing in a JT valve to a pressure slightly above atmospheric [6]. LNG is then obtained. In the MR loop, the superheated MR leaving the MHEX undergoes a multi-stage compression process with intercooling to attain high pressure (In Figure 3, two, three, and four compression stages are shown). The generated high pressure MR stream also enters MHEX as another hot stream. Upon exiting, its pressure is reduced as it passes through a JT valve, thereby creating the cold MR stream. This is vaporized in the MHEX to form superheated MR, and hence completing the cycle.

3 Modelling and optimization

3.1 Mathematical modelling

The discharge pressure for any stage i in multistage compression for a total number of compressors K is given by;

$$P_i = \mathcal{PR}^i P_{min} \qquad i \in \{1, 2, ..., K\} \tag{1}$$

The stage pressure ratio $\mathcal{PR}$ is estimated using $\mathcal{PR} = (\frac{P_{max}}{P_{min}})^{1/K}$ where P_{min} is the minimum pressure and P_{max} the maximum pressure.

The Peng-Robinson equation of state is utilized for the calculation of thermodynamic quantities. This choice of equation of state is made due to its suitability for non-polar and moderately polar mixtures. Moreover, it exhibits efficient computational performance, particularly near critical conditions [14].

3.1.1 Compressor

The equations that govern the performance of the compressor are cited from Matovu et al. [34] and can be summarized as follows:

The isentropic temperature T_{is} is obtained using Eqn (2), where R represents the universal gas constant.

$$T_{is} = T_{in}(\frac{P_{out}}{P_{in}})^{\frac{R}{Cp_{av}}} \tag{2}$$

In the above Eqn (2), the average specific heat capacity, Cp_{av}, is computed at the mean temperature of the compressor. All specific heat capacities are calculated using the Aly-Lee model [35].

Eqn (3) is used to determine the index of compression, n_k:

$$n_k = \frac{\ln(P_{out}/P_{in})}{\ln(\nu_{in}/\nu_{out})} \equiv \frac{\ln(P_{out}/P_{in})}{\ln((T_{in}/P_{in})/(T_{is}/P_{out}))} \tag{3}$$

Here, ν_{in} is the specific inlet volume and ν_{out} the specific outlet volume of gas.

The temperature of the stream exiting the compressor, T_{out}, is calculated using Eqn (4).

$$T_{out} = T_{in}(\frac{P_{out}}{P_{in}})^{(\frac{n_k-1}{n_k\eta_p})} \tag{4}$$

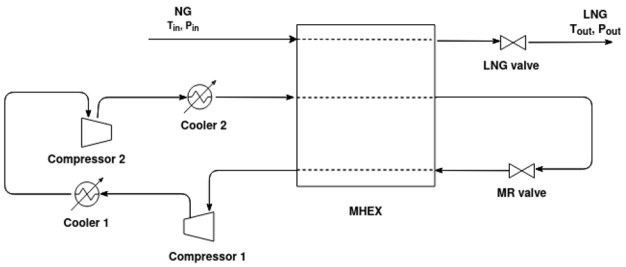

(a) Configuration 1: Two compression stages.

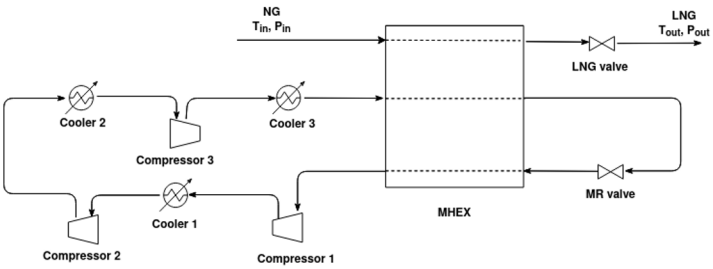

(b) Configuration 2: Three compression stages.

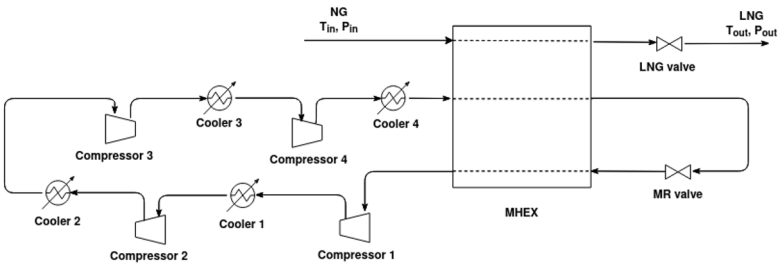

(c) Configuration 3: Four compression stages.

Figure 3: Different compressor configurations for the SMR process.

where η_p the polytropic efficiency.

The polytropic head factor f_p is given by Eqn (5).

$$f_p = \left(\frac{h_{is,out} - h_{in}}{RT_{is} - RT_{in}}\right)\left(\frac{n_k - 1}{n_k}\right) \tag{5}$$

Here, h_{in} and $h_{is,out}$ are the specific inlet and specific isentropic discharge enthalpies, respectively.

The polytropic head, $\mathcal{H}$, is defined as given by Eqn (6). The term $\frac{g.MW}{1000}$ is a correction term to convert $\mathcal{H}$ to meters (m).

$$\mathcal{H} = f_p RT_{in} \frac{n_k \eta_p}{n_k - 1} [(\frac{P_{out}}{P_{in}})^{(\frac{n_k - 1}{n_k \eta_p})} - 1] / (\frac{g.MW}{1000}) \tag{6}$$

The shaft work of the compressors is then determined as given by Eqn (7).

$$w = \frac{m(\frac{g.MW}{1000})\mathcal{H}}{\eta_p \eta_m} \tag{7}$$

Here, m represents the molar flow rate into the compressor, and η_m is the mechanical efficiency.

3.1.2 Cooler

The equation that governs performance of the cooler is as follows. The heat transfer rate or duty Q is calculated using the equation:

$$Q = m(h_{in} - h_{out}) \tag{8}$$

Here, m is the molar flow rate, and h_{in} and h_{out} denote the molar enthalpies of the incoming and outgoing streams, respectively. These enthalpies depend on the composition, temperature, and pressure of the respective streams. The actual enthalpy is a summation of the enthalpy departure and the ideal enthalpy. The departure enthalpy is calculated based on the Peng-Robinson equation of state. The necessary equations are obtained from Dahm and Visco [36].

3.2 The generalized disjunctive programming model

The generalized disjunctive programming (GDP) model formulation is given by Eqn (9).

$$\begin{aligned}
\min\ & z = f(x) \\
\text{s.t.}\ & g(x) \le 0, \\
& \bigvee_{d \in D_k} \begin{bmatrix} Y_{kd} \\ E_{kd}(x) \le 0 \end{bmatrix}, \quad k \in K, \\
& \underline{\vee}_{d \in D_k}\ Y_{kd}, \quad k \in K \\
& \Omega(Y) = \text{True}, \\
& x^{lo} \le x \le x^{up} \\
& x \in \mathbb{R}^q \\
& Y_{kd} \in \{\text{True}, \text{False}\}, k \in K, d \in D_k
\end{aligned} \tag{9}$$

Here, the continuous variables are denoted as x, with x^{lo} representing the lower bounds and x^{up} the upper bounds associated with these variables. The objective function is denoted as $f(x)$, and the variables Y_{kd} are of boolean nature. The expression $g(x) \le 0$ represents global

constraints, which are always true, irrespective of the specific discrete choices made. In this context, square brackets indicate disjunctions, where each disjunction k signifies significant discrete decisions. The disjuncts d within each disjunction represents various selection alternatives. When the boolean variable Y_{kd} is $True$, the constraints $E_{kd}(x) \leq 0$ are considered valid; otherwise, they are not valid. It's important to note that for each disjunction, only one of the disjuncts can be True. The constraints $\Omega(Y) = \text{True}$ define the logical connections among the boolean variables.

3.3 The GDP model applied to multistage compression involving K compression stages

The GDP model given by Eqn (10) comprises of various components. These include an objective function that aims to minimize the overall shaft work requirement. Furthermore, it includes global constraints that apply universally, irrespective of the particular disjuncts selected from each disjunction. The model is further structured with K disjunctions spanning from 0 to $K-1$. The disjunction is the major discrete decision that represents selection of a pressure level k. The disjuncts in each disjunction represent selection alternatives to a higher pressure level d. Hence for the selection to be valid, $d \geq k$.

$$
\begin{aligned}
&\min \ W = \sum_{k \in K} \sum_{d \in D_k} w_{kd} \\
&\text{s.t.} \quad g(x) \leq 0, \\
&\begin{bmatrix} Y_{0,0} \\ E_{0,0}(x) \leq 0 \\ W_0 = w_{0,0} \end{bmatrix} \vee \begin{bmatrix} Y_{0,1} \\ E_{0,1}(x) \leq 0 \\ W_0 = w_{0,1} \end{bmatrix} \vee \begin{bmatrix} Y_{0,2} \\ E_{0,2}(x) \leq 0 \\ W_0 = w_{0,2} \end{bmatrix} \vee \ldots \begin{bmatrix} Y_{0,K} \\ E_{0,K}(x) \leq 0 \\ W_0 = w_{0,K} \end{bmatrix} \\
&\begin{bmatrix} Y_{1,1} \\ E_{1,1}(x) \leq 0 \\ W_1 = w_{1,0} \end{bmatrix} \vee \begin{bmatrix} Y_{1,2} \\ E_{1,2}(x) \leq 0 \\ W_1 = w_{1,2} \end{bmatrix} \vee \ldots \begin{bmatrix} Y_{1,K} \\ E_{1,K}(x) \leq 0 \\ W_1 = w_{1,K} \end{bmatrix} \\
&\quad \vdots \qquad\qquad \vdots \qquad\qquad \vdots \\
&\begin{bmatrix} Y_{K-1,K-1} \\ E_{K-1,K-1}(x) \leq 0 \\ W_K = w_{K-1,K-1} \end{bmatrix} \vee \begin{bmatrix} Y_{K-1,K} \\ E_{K-1,K}(x) \leq 0 \\ W_K = w_{K-1,K} \end{bmatrix} \\
&\underset{d \in D_k}{\vee} Y_{kd}, \quad \forall k \in K \\
&x \in X \\
&k \in \{0, 1, ..., K\} \\
&Y_{k,d} \in \{\text{True}, \text{False}\}, \ \forall k \in K, \ d \in D_k; \ d \geq k
\end{aligned}
\tag{10}
$$

3.3.1 Objective function

The objective is to reduce the overall shaft work requirement to a minimum through strategic selection of stages. The model's equation is presented as Eqn (11).

$$
W = \sum_{k \in K} \sum_{d \in D_k} w_{kd} \tag{11}
$$

Here, W denotes the total shaft work, and w_{kd} signifies the shaft work demand of the compressor from pressure level k to d. Thus,

$$w_{kd} = \frac{m(\frac{g.MW}{1000})\mathcal{H}_{kd}}{\eta_p \eta_m} \tag{12}$$

where $\mathcal{H}_{kd}$ is the polytropic head of a compressor from level k to d.

3.3.2 Global constraints

The discharge pressure of compressor k to d should be similar to pressure level d.

$$P_{kd,out} = P_d \tag{13}$$

The multiplication of pressure ratios across all stages results in the total pressure ratio, a constant value since the minimum and maximum pressures are constant.

$$\prod_{k=1}^{K} \mathcal{PR}_{k-1,k} = \mathcal{PR}_{tot} \tag{14}$$

3.3.3 Equality constraints

The equality constraints are model equations presented in section 3.1.

3.3.4 Inequality constraints

The compressor outlet pressures are restricted between the minimum and maximum pressures.

$$P_{kd,out} \geq P_{min} \quad \text{and} \quad P_{kd,out} \leq P_{max} \tag{15}$$

The pressure ratios are bounded between 1.0 and total presuure ratio $\mathcal{PR}_{tot}$ respectively.

$$\mathcal{PR}_{kd} \geq 1.0 \quad \text{and} \quad \mathcal{PR}_{kd} \leq \mathcal{PR}_{tot} \tag{16}$$

The outlet temperatures of compressor level k to d can not exceed the maximum temperature $T_{max,out}$, thus

$$T_{kd,out} \leq T_{max,out} \tag{17}$$

4 Results and discussion

4.1 Case studies: Multistage compression for a single mixed refrigerant process

These case studies consider optimization of the compressor configurations of SMR process. The configurations composed of two, three and four compressors respectively are denoted Config.1, 2, and 3. The data for the process is obtained from Tak et al. [18]. The natural gas parameters for the configurations are shown in Table 1. The MR and other parameters are in shown in Table 2. The objective is to find a set of pressure levels that, when combined, minimize the shaft work required while still satisfying process constraints. The natural gas parameters and refrigerant flow rates and compositions are maintained constant. The lowest and highest pressures P_0, P_K are considered constant to meet process requirements.

Table 1: Natural gas parameters for the SMR processes with different compressor configurations.

Parameter	Config.1	Config.2	Config.3
natural gas flow rate (kg/s)	1.0	1.0	1.0
natural gas temperature (K)	298.15	298.15	298.15
natural gas pressure (bar)	55.0	55.0	55.0
natural gas composition (mol %)			
methane	91.3	82.0	82.0
ethane	5.4	11.2	11.2
propane	2.1	4.0	4.0
i-butane	0.5	1.2	1.2
n-butane	0.5	0.9	0.9
nitrogen	0.2	0.7	0.7

Table 2: Mixed refrigerant and other parameters for the SMR processes with different compressor configurations.

Parameter	Config. 1	Config. 2	Config. 3
mixed refrigerant flow rate (mol/s)	165.4	158.7	176.0
mixed refrigerant composition (mol %)			
methane	23.8	25.1	25.5
ethane	35.7	32.6	32.2
propane	0.1	0.8	1.4
i-butane	4.5	3.8	2.7
n-butane	21.9	21.8	22.1
nitrogen	14.0	15.9	16.1
Inlet temperature of compressor 1 (K)	300.05	300.15	300.15
Inlet pressure of compressor 1 (bar)	3.35	4.26	4.72
Compression ratio			
compressor #1	3.19	1.66	1.35
compressor #2	2.78	1.60	1.41
compressor #3		2.91	1.28
compressor #4			2.60

$$
\begin{aligned}
&\min\ \mathbb{W} = \sum_{k\in K}\sum_{d\in D_k} w_{kd} \\
&\text{s.t.}\quad g(x) \le 0, \\
&\begin{bmatrix} Y_{0,0} \\ E_{0,0}(x) \le 0 \\ W_0 = w_{0,0} \end{bmatrix} \vee \begin{bmatrix} Y_{0,1} \\ E_{0,1}(x) \le 0 \\ W_0 = w_{0,1} \end{bmatrix} \vee \begin{bmatrix} Y_{0,2} \\ E_{0,2}(x) \le 0 \\ W_0 = w_{0,2} \end{bmatrix} \vee \begin{bmatrix} Y_{0,3} \\ E_{0,3}(x) \le 0 \\ W_0 = w_{0,3} \end{bmatrix} \\
&\begin{bmatrix} Y_{1,1} \\ E_{1,1}(x) \le 0 \\ W_1 = w_{1,0} \end{bmatrix} \vee \begin{bmatrix} Y_{1,2} \\ E_{1,2}(x) \le 0 \\ W_1 = w_{1,2} \end{bmatrix} \vee \begin{bmatrix} Y_{1,3} \\ E_{1,3}(x) \le 0 \\ W_1 = w_{1,3} \end{bmatrix} \\
&\begin{bmatrix} Y_{2,2} \\ E_{2,2}(x) \le 0 \\ W_2 = w_{2,2} \end{bmatrix} \vee \begin{bmatrix} Y_{2,3} \\ E_{2,3}(x) \le 0 \\ W_2 = w_{2,3} \end{bmatrix} \\
&Y_{0,0} \veebar Y_{0,1} \veebar Y_{0,2} \veebar Y_{0,3} \\
&Y_{1,1} \veebar Y_{1,2} \veebar Y_{1,3} \\
&Y_{2,2} \veebar Y_{2,3} \\
&x \in \{P_0, P_1, P_2, P_3\} \\
&Y_{k,d} \in \{\text{True}, \text{False}\},\ \forall k \in K,\ d \in D_k;\ d \ge k \\
&k, d \in \{0, 1, 2, 3\}
\end{aligned}
\tag{18}
$$

The GDP model for a sample case of three (3) compression stages (K=3) is given by Eqn (18). Note that the disjuncts with $k = d$ imply that the same pressure level is selected. This is not a desired operation. All GDP models for the different K values (K=2, K=3, and K=4) are implemented in Python 3.8.16 using Pyomo [37] and their properties are shown in Table 3.

Table 3: The GDP model properties for different compressor configurations.

Property	Config.1 (K2)	Config.2 (K3)	Config.3 (K4)
Disjunctions	2	3	4
Disjuncts	5	9	14
Constraints	27	46	70
Variables	27	47	72
continuous	22	38	58
binary	5	9	14
integer	0	0	0

The model's discharge pressures are constrained to fall within the range of P_{min} to P_{max}, while temperatures are limited between 298.15 K and 420.0 K. An extension to Pyomo algebraic modelling language called Pyomo.GDP [38] is employed to formulate the GDP models. The Logic-Based Branch and Bound (GDPopt-LBB) strategy [39] of the GDPopt solver within Pyomo.GDP is utilized, with SCIP [40] serving as the MINLP subsolver to solve these models. The computations are conducted on a system with an Intel®core i7 CPU 2.80 GHz with 16GB of RAM, operating Ubuntu 22.04.2 LTS. Remarkably, the results are obtained in a few seconds.

Furthermore, the GDP model results are validated through simulations conducted with Aspen Hysys software. The compressor discharge pressures are used with parameters given in Tables 1 and 2 for the simulations. The SMR process configurations depicted in Figures 3a, 3b, and 3c have been simulated using Aspen Hysys, and the property package utilized for the simulation is the Peng-Robinson equation of state. The polytropic efficiencies are assumed to be 0.8205, 0.8135, and 0.813 for K=2, K=3, and K=4 models respectively. All coolers are assumed to have no pressure drop.

Table 4 shows all summarized results. The RR results are referenced from Tak et al. [18]. They result from implementation of optimization of SMR processes in gPROMS using the successive reduced quadratic programming solver. These are resimulated using Aspen Hysys to obtained the base case (BC) results in the Table 4. The GM results are obtained by solving the GDP models presented in this work.

For the two stage case, the optimal interstage pressure obtained using GM increases from 10.69 to 11.00 bar in reference to the base case. This results in a larger shaft work w_1 but lower shaft work w_2. The overall is a reduced total shaft work w_{tot} of 1130.1 kW. For the three stage case, the optimal interstage pressure GM results are 8.26 and 16.32 bar respectively. They are greater than the BC results of 7.072 and 11.32 bar. The combined effect is a total shaft work w_{tot} of 988.2 kW a reduction from the base case value of 992.6 kW. For the four stage case, the optimal interstage pressure GM results are 7.34, 12.00 and 19.00 bar. They are greater than the BC results of 6.372, 8.985 and 11.52 bar. The combined effect is a total shaft work w_{tot} of 970.0 kW a reduction from the base case value of 982.1 kW.

The AH results are obtained from Aspen Hysys for validation purposes, after simulation of GM results. This is to ensure that the results obtained from the GDP models are reliable and comparable to those obtained from a universally acceptable commercial software. For

the two stage case, the AH total shaft work is 1130.1 kW with a difference of 0.0% from the GM result of 1130.1 kW. For the three stage case, the AH total shaft is 988.5 kW with a difference of 0.03% from the GM result of 988.2 kW. For the four stage case, the AH total shaft is 970.7 kW with a difference of 0.07% from the GM result of 970.0 kW. It is clear that all the differences are within acceptable limits and hence the GM results are reliable. In terms of shaft work savings, the two stage case results in savings of atmost 0.0088 % against the base case. For the three stage case, savings of 0.4433 and 0.4131 % are obtained against the base case for GM and AH results respectively. Savings of 1.2321 and 1.1608 % are obtained for the four stage case for GM and AH results respectively. It's evident that the savings increase with increasing number of stages. These are significant savings since such processes are energy intensive that even a small reduction results in huge cost savings. In addition, the savings are obtained on already optimized base case scenarios referenced from Tak et al. [18].

Table 4: The comparison of optimization results using different models and simulation. RR-Reference, BC-Base case, GM -GDP model, AH-Aspen HYSYS.

Variable	Config. 1 (two stage)				Config. 2 (three stage)				Config. 3 (four stage)			
	RR	BC	GM	AH	RR	BC	GM	AH	RR	BC	GM	AH
Pressure P_0 (bar)	3.35	3.35	3.35	3.35	4.26	4.26	4.26	4.26	4.72	4.72	4.72	4.72
Pressure P_1 (bar)	10.69	10.69	11.00	11.00		7.072	8.26	8.26		6.372	7.34	7.34
Pressure P_2 (bar)		29.71	29.71	29.71	11.32	11.32	16.32	16.32		8.985	12.00	12.00
Pressure P_3 (bar)						32.94	32.94	32.94	11.52	11.52	19.00	19.00
Pressure P_4 (bar)										29.95	29.95	29.95
Shaft work w_1 (KW)	622.7	622.1	639.2	638.8	249.0	248.8	329.1	329.1	160.4	160.2	238.5	238.6
Shaft work w_2 (KW)	507.5	508.1	490.9	491.3	228.4	226.9	330.3	330.3	184.3	183.6	263.3	263.4
Shaft work w_3 (KW)					514.8	516.9	328.8	329.1	128.9	128.8	235.4	235.6
Shaft work w_4 (KW)									508.9	509.5	232.8	233.1
Total shaft work w_{tot} (KW)	1130.2	1130.2	1130.1	1130.1	992.2	992.6	988.2	988.5	982.5	982.1	970.0	970.7
Savings (%)	-	-	0.0088	0.0088	-	-	0.4433	0.4131	-	-	1.2321	1.1608

Furthermore, Aspen Hysys simulations are utilized to extract the results of multistream heat exchangers. Subsequently, these results are employed to generate the composite curves showcased in Figures 4, 5, and 6. These curves exhibit characteristic shapes indicative of the SMR process, featuring minimal temperature differences for low temperatures between 113.15 K and 200 K, and more pronounced temperature variations at higher temperatures, exceeding 225 K. Upon close examination of Figures 4, 5, and 6, it becomes evident that there is no overlap or intersection between the hot and cold composite curves. Hence, signifying the feasibility of heat transfer. Within these figures, the "Hot MR" corresponds to the high pressure mixed refrigerant streams within the heat exchangers. When combined with the natural gas streams, they form the hot streams, thereby forming the hot composite curves. Conversely, the "Cold MR" corresponds to the low pressure mixed refrigerant streams and serves as the cold streams within the heat exchangers. These cold MR streams align with the cold composite curves in the same graphs, indicating their collinearity. The gap observed between the hot and cold composite curves in all three Figures 4, 5, and 6 is associated with the shaft work consumption. Specifically, the largest gap, as depicted in Figure 4, corresponds to the highest shaft work consumption, while the smallest gap, as evident in Figure 6, signifies the lowest shaft work consumption.

The proposed GDP model implemented on the optimized referenced literature cases results in shaft work savings of atmost 0.0088%, 0.4433%, and 1.2321%; obtained for the two, three, and four stage compression systems respectively. The optimized cases also result in feasible SMR processes based on the composite curves as depicted in Figures 4, 5 and 6.

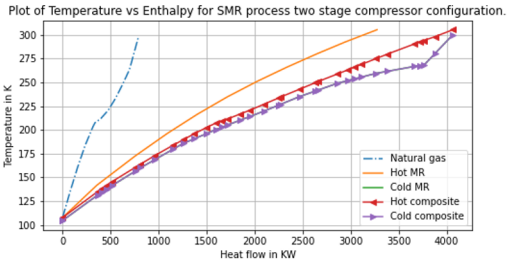

Figure 4: The composite curves for two compressor configuration SMR process.

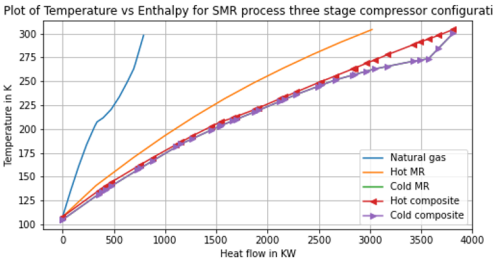

Figure 5: The composite curves for three compressor configuration SMR process.

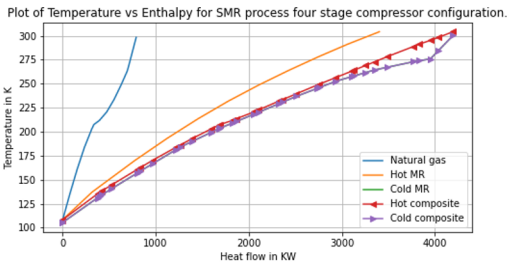

Figure 6: The composite curves for four compressor configuration SMR process.

This points to effectiveness of the GDP approach for optimizing mixed integer (discrete-continuous) optimization problems.

5 Conclusion

A generalized disjunctive programming model for multistage compression is developed in this work. The model is useful for both synthesis and optimization of multistage compression configurations. By using this approach, we further seek improvements in shaft work savings. The GDP models are formulated in the Pyomo modeling language and solved using the GDPopt solver, which utilizes the Logic-Based Branch and Bound (GDPopt-LBB) approach, with SCIP serving as a subsolver. This approach enhances convergence and solution speed, hence solving the models in a few seconds. This enables us to effectively and efficiently solve difficult mixed integer optimization problems. The methodology is applied on a case study of multistage compression for a prior optimized SMR process obtained from literature. Aspen Hysys software is used for simulation to validate the model results. The optimization results yield shaft work savings of atmost 0.0088%, 0.4433%, and 1.2321% for the two, three, and four stage compression systems respectively against the optimized base cases from literature. The results demonstrate that the proposed model is not only useful for synthesis and optimization but also improves on shaft work savings of already optimized cases.

References

[1] R. Ahmed, S. Mahadzir, N. E. B. Rozali, K. Biswas, F. Matovu, and K. Ahmed, "Artificial intelligence techniques in refrigeration system modelling and optimization: A multi-disciplinary review," *Sustainable Energy Technologies and Assessments*, vol. 47, p. 101488, 2021.

[2] M. A. Pereira, L. F. Santos, J. A. Caballero, M. A. Ravagnani, and C. B. Costa, "Energy and economic comparison of five mixed-refrigerant natural gas liquefaction processes," *Energy Conversion and Management*, vol. 272, p. 116364, 2022.

[3] S. Jarungthammachote, "Optimal interstage pressures of multistage compression with intercooling processes," *Thermal Science and Engineering Progress*, vol. 29, p. 101202, 2022.

[4] H. Lugo-Méndez, T. Lopez-Arenas, A. Torres-Aldaco, E. V. Torres-González, M. Sales-Cruz, and R. Lugo-Leyte, "Interstage pressures of a multistage compressor with intercooling," *Entropy*, vol. 23, no. 3, p. 351, 2021.

[5] R. Ahmed, S. Mahadzir, A. Mota-Babiloni, M. Al-Amin, A. Y. Usmani, Z. Ashraf Rana, H. Yassin, S. Shaik, and F. Hussain, "4e analysis of a two-stage refrigeration system through surrogate models based on response surface methods and hybrid grey wolf optimizer," *PloS one*, vol. 18, no. 2, p. e0272160, 2023.

[6] Muhammad Abdul Qyyum, Q. Kinza, and M. Lee, "Comprehensive Review of the Design Optimization of Natural Gas Liquefaction Processes: Current Status and Perspectives," 2018.

[7] R. Ahmed, G. P. Rangaiah, S. Mahadzir, S. Mirjalili, M. H. Hassan, and S. Kamel, "Memory, evolutionary operator, and local search based improved grey wolf optimizer with linear population size reduction technique," *Knowledge-Based Systems*, p. 110297, 2023.

[8] M. S. Khan, S. Lee, and M. Lee, "Optimization of single mixed refrigerant natural gas liquefaction plant with nonlinear programming," *Asia-Pacific Journal of Chemical Engineering*, vol. 7, pp. S62–S70, 2012.

[9] P. E. Wahl, S. W. Løvseth, and M. J. Mølnvik, "Optimization of a simple lng process using sequential quadratic programming," *Computers & chemical engineering*, vol. 56, pp. 27–36, 2013.

[10] J.-H. Hwang, M.-I. Roh, and K.-Y. Lee, "Determination of the optimal operating conditions of the dual mixed refrigerant cycle for the lng fpso topside liquefaction process," *Computers & Chemical Engineering*, vol. 49, pp. 25–36, 2013.

[11] S. F. Mussati, S. Cignitti, S. S. Mansouri, K. V. Gernaey, T. Morosuk, and M. C. Mussati, "Configuration optimization of series flow double-effect water-lithium bromide absorption refrigeration systems by cost minimization," *Energy Conversion and Management*, vol. 158, pp. 359–372, 2018.

[12] M. M. H. Shirazi and D. Mowla, "Energy optimization for liquefaction process of natural gas in peak shaving plant," *Energy*, vol. 35, no. 7, pp. 2878–2885, 2010.

[13] M. S. Khan and M. Lee, "Design optimization of single mixed refrigerant natural gas liquefaction process using the particle swarm paradigm with nonlinear constraints," *Energy*, vol. 49, pp. 146–155, 2013.

[14] E. Primabudi, T. Morosuk, and G. Tsatsaronis, "Multi-objective optimization of propane pre-cooled mixed refrigerant (C3MR) LNG process," *Energy*, vol. 185, pp. 492–504, 2019.

[15] A. Alabdulkarem, A. Mortazavi, Y. Hwang, R. Radermacher, and P. Rogers, "Optimization of propane pre-cooled mixed refrigerant lng plant," *Applied thermal engineering*, vol. 31, no. 6-7, pp. 1091–1098, 2011.

[16] A. Aspelund, T. Gundersen, J. Myklebust, M. P. Nowak, and A. Tomasgard, "An optimization-simulation model for a simple lng process," *Computers & Chemical Engineering*, vol. 34, no. 10, pp. 1606–1617, 2010.

[17] F. Almeida-Trasvina, R. Smith, and M. Jobson, "Development of an energy-efficient single mixed refrigerant cycle for small-scale lng production," *Industrial & Engineering Chemistry Research*, vol. 60, no. 32, pp. 12049–12067, 2021.

[18] K. Tak, I. Lee, H. Kwon, J. Kim, D. Ko, and I. Moon, "Comparison of multistage compression configurations for single mixed refrigerant processes," *Industrial & Engineering Chemistry Research*, vol. 54, no. 41, pp. 9992–10000, 2015.

[19] A. Ebrahimi, J. Tamnanloo, S. H. Mousavi, E. Soroodan Miandoab, E. Hosseini, H. Ghasemi, and S. Mozaffari, "Discrete-continuous genetic algorithm for designing a mixed refrigerant cryogenic process," *Industrial & Engineering Chemistry Research*, vol. 60, no. 20, pp. 7700–7713, 2021.

[20] G. C. Lee, R. Smith, and X. X. Zhu, "Optimal synthesis of mixed-refrigerant systems for low-temperature processes," *Ind. Eng. Chem. Res.*, vol. 41, no. 20, pp. 5016–5028, 2002.

[21] T. He, Z. Liu, Y. Ju, and A. M. Parvez, "A comprehensive optimization and comparison of modified single mixed refrigerant and parallel nitrogen expansion liquefaction process for small-scale mobile lng plant," *Energy*, vol. 167, pp. 1–12, 2019.

[22] A. H. Aslambakhsh, M. A. Moosavian, M. Amidpour, M. Hosseini, and S. AmirAfshar, "Global cost optimization of a mini-scale liquefied natural gas plant," *Energy*, vol. 148, pp. 1191–1200, 2018.

[23] I. Lee and I. Moon, "Total cost optimization of a single mixed refrigerant process based on equipment cost and life expectancy," *Industrial & Engineering Chemistry Research*, vol. 55, no. 39, pp. 10336–10343, 2016.

[24] Q. Li and Y. Ju, "Design and analysis of liquefaction process for offshore associated gas resources," *Applied Thermal Engineering*, vol. 30, no. 16, pp. 2518–2525, 2010.

[25] K. Qadeer, M. A. Qyyum, and M. Lee, "Krill-herd-based investigation for energy saving opportunities in offshore liquefied natural gas processes," *Industrial & Engineering Chemistry Research*, vol. 57, no. 42, pp. 14162–14172, 2018.

[26] M. A. Qyyum, N. V. D. Long, M. Lee, *et al.*, "Design optimization of single mixed refrigerant lng process using a hybrid modified coordinate descent algorithm," *Cryogenics*, vol. 89, pp. 131–140, 2018.

[27] R. Raman and I. E. Grossmann, "Modelling and computational techniques for logic based integer programming," *Computers and Chemical Engineering*, vol. 18, no. 7, pp. 563–578, 1994.

[28] F. Trespalacios and I. E. Grossmann, "Chapter 24: Review of Mixed-Integer Nonlinear Optimization and Generalized Disjunctive Programming Applications in Process Systems Engineering," *Advances and Trends in Optimization with Engineering Applications*, pp. 315–329, 2017.

[29] Q. Chen and I. Grossmann, "Modern modeling paradigms using generalized disjunctive programming," *Processes*, vol. 7, no. 11, 2019.

[30] Q. Chen and I. E. Grossmann, "Effective Generalized Disjunctive Programming Models for Modular Process Synthesis," *Industrial and Engineering Chemistry Research*, vol. 58, pp. 5873–5886, apr 2019.

[31] F. Matovu, S. Mahadzir, R. Ahmed, and N. E. M. Rozali, "Synthesis and optimization of multilevel refrigeration systems using generalized disjunctive programming.," *Computers & Chemical Engineering*, p. 107856, 2022.

[32] F. D. Nogal, J.-K. Kim, S. Perry, and R. Smith, "Optimal design of mixed refrigerant cycles," *Industrial & Engineering Chemistry Research*, vol. 47, no. 22, pp. 8724–8740, 2008.

[33] I. López-Paniagua, J. Rodríguez-Martín, S. Sánchez-Orgaz, and J. J. Roncal-Casano, "Step by step derivation of the optimum multistage compression ratio and an application case," *Entropy*, vol. 22, no. 6, p. 678, 2020.

[34] F. Matovu, S. Mahadzir, N. E. Mohammad Rozali, and C. Yoke Yi, "Analysis and optimization of multistage mixed refrigerant systems using generalized disjunctive programming," *Process Integration and Optimization for Sustainability*, pp. 1–16, 2023.

[35] F. A. Aly and L. L. Lee, "Self-consistent equations for calculating the ideal gas heat capacity, enthalpy, and entropy," *Fluid Phase Equilibria*, vol. 6, no. 3-4, pp. 169–179, 1981.

[36] K. D. Dahm and D. P. Visco, *Fundamentals of chemical engineering thermodynamics*. Cengage Learning, 2014.

[37] W. E. Hart, C. D. Laird, J.-P. Watson, D. L. Woodruff, G. A. Hackebeil, B. L. Nicholson, and J. D. Siirola, *Pyomo-optimization modeling in python*, vol. 67. Springer, 2017.

[38] Q. Chen, E. S. Johnson, J. D. Siirola, and I. E. Grossmann, "Pyomo.GDP: Disjunctive Models in Python," *Computer Aided Chemical Engineering*, vol. 44, pp. 889–894, 2018.

[39] Q. Chen, E. S. Johnson, D. E. Bernal, R. Valentin, S. Kale, J. Bates, J. D. Siirola, and I. E. Grossmann, "Pyomo.GDP: an ecosystem for logic based modeling and optimization development," *Optimization and Engineering*, pp. 1–36, apr 2021.

[40] S. Vigerske and A. Gleixner, "SCIP: global optimization of mixed-integer nonlinear programs in a branch-and-cut framework," *Optimization Methods and Software*, vol. 33, no. 3, pp. 563–593, 2018.